

Influence of measurement on the life-time and the line-width of unstable systems

Brahim Elattari^{1,2} and S.A. Gurvitz³

¹Departamento de física Teórica de la Materia Condensada, Universidad Autónoma de Madrid, Cantoblanco, Madrid 28049, Spain

²Université Chouaïb Doukkali, Faclté des Sciences, El Jadida, Morocco

³Weizmann Institute of Science, Department of Particle Physics
76100 Rehovot, Israel

We investigate the quantum Zeno effect in the case of electron tunneling out of a quantum dot in the presence of continuous monitoring by a detector. It is shown that the Schrödinger equation for the whole system can be reduced to Bloch-type rate equations describing the combined time-development of the detector and the measured system. Using these equations we find that continuous measurement of the unstable system does not affect its exponential decay to a reservoir with a constant density of states. The width of the energy distribution of the tunneling electron, however, is not equal to the inverse life-time – it increases due to the decoherence generated by the detector. We extend the analysis to the case of a reservoir described by an energy dependent density of states, and we show that continuous measurement of such quantum systems affects both the exponential decay rate and the energy distribution. The decay does not always slow down, but might be accelerated. The energy distribution of the tunneling electron may reveal the lines invisible before the measurement.

PACS: 73.23.Hk.03.65.Bz.73.23.-b

I. INTRODUCTION

The interplay between quantum dynamics and quantum measurements has attracted much attention of physicists since the discovery of quantum mechanics. In fact, it was suggested that frequent or continuous observations of an unstable quantum system can inhibit or slow down its decay [1]. This phenomenon is known as the quantum Zeno effect. Usually this effect is associated to von Neumann's postulate in the theory of quantum measurements [2]. Indeed, in the classical example of two-level systems, the probability of a quantum transition from an initially occupied unstable state is given at short time, Δt , by $P(\Delta t) = a(\Delta t)^2$. If we assume that Δt is the measurement time, which consists in projecting the system onto the initial state, then after N successive measurements the probability of finding the unstable system in its initial state, at time $t = N\Delta t$, is $Q(t) = [1 - a(\Delta t)^2]^{(t/\Delta t)}$. It follows from this result that $Q(t) \rightarrow 1$ for $\Delta t \rightarrow 0$, i.e. suppression of quantum transition.

During last years the Zeno effect has become a topic of great interest. It has been discussed in the areas of radioactive decay [3], polarized light [4], the physics of atoms [5,6], neutron physics [7], quantum optics [8,9] and mesoscopic physics [10–12]. As a matter of fact, the theoretical and experimental efforts has been mainly concentrated on quantum transitions between isolated levels [15] characterized by an oscillatory behavior. In this latter case the slowing down of the transition rate has, indeed, been found. However, this was attributed to the decoherence generated by the detector without an explicit

involvement of the projection postulate [16,10]. On the other hand, the slowing down of the exponential decay rate still remains a controversial issue, despite the fact that it is extensively studied [17–21] and further investigations are clearly desirable.

In this paper we focus our attention on observation of spontaneous decay using a microscopic description of the measurement device (detector). The latter point should be very essential in any investigations of measurement problems. The quantum-mechanical description of the measurement device would allow us to study thoroughly the measurement process without explicit use of the projection postulate, or introducing different phenomenological terms in quantum evolution of the measured system. Yet, the detector is a macroscopic system, the quantum mechanical analysis of which is very complicated. Thus one can expect that mesoscopic systems, which are between the microscopic and macroscopic scales, would be very useful for this type of investigation [22]. In addition, the actual experimental investigations of the quantum Zeno effect in mesoscopic systems are within reach of nowadays experimental techniques.

Our quantum-mechanical treatment of the entire system, including the detector is based on the new Bloch-type rate equations, which we derived here from the many-body Schrödinger equation. These equations would allow us to trace the quantum-mechanical behavior of the entire measured system during the measurement. In contrast with the standard Bloch equations, our equations describe the reservoir states too. As a result, we can find the influence of the measurement on the energy distribution of the decayed system, as well as its time-evolution.

The paper is organized as follows: In Sect. 2 we gave a general quantum-mechanical description of an unstable system. We concentrated on conditions under which an exponential and non-exponential decay can be obtained, yet without including any measurement apparatus. The latter is introduced in Sect. 3 where we derive the rate equations, describing the dynamical evolution of the measurement process. The results of our analysis are described in Sect. 4. The last section is a summary. Some of the results described in this paper were presented in [12].

II. DYNAMICS OF A DECAYED SYSTEM

Let us consider a mesoscopic quantum dot coupled to an electron reservoir on its right, Fig. 1. We assume only one level, E_0 , inside the quantum dot, Fig. 1. The system is described by the following tunneling Hamiltonian written in the occupation number representation:

$$H_{QD} = E_0 c_0^\dagger c_0 + \sum_{\alpha} E_{\alpha} c_{\alpha}^\dagger c_{\alpha} + \sum_{\alpha} [\Omega_{\alpha} c_{\alpha}^\dagger c_0 + H.c.]. \quad (1)$$

Here the operators $c_{\alpha}^{\dagger}(c_{\alpha})$ correspond to the creation (annihilation) of an electron in state α in the reservoir, and the operator $c_0^{\dagger}(c_0)$ is similarly defined for the state in the quantum dot. The Ω_{α} are the hopping amplitudes between the states E_0, E_{α} . (We choose the gauge, where Ω_{α} are real). This Hamiltonian (1) does not include any coupling with radiation or phonon fields as had been done for example in [13,14].

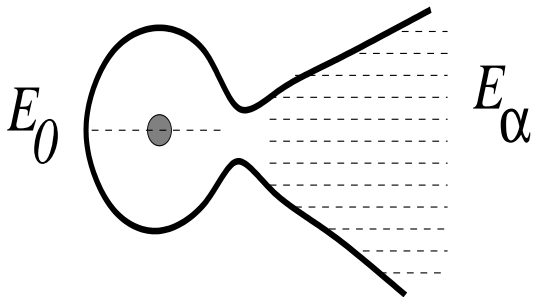


Fig. 1: The energy level E_0 of the dot occupied by an electron, which tunnels to continuous states E_{α} of the reservoir.

The initial state of the entire system $c_0^{\dagger}|0\rangle$ corresponds to occupied quantum dot and empty states in the reservoir. This state is unstable: the Hamiltonian (1) requires it to decay to the continuum states $c_{\alpha}^{\dagger}|0\rangle$ having the electron in the reservoir. The electron wave function, describing its evolution can be written in the most general way as

$$|\Psi(t)\rangle = \left[b_0(t)c_0^{\dagger} + \sum_{\alpha} b_{\alpha}(t)c_{\alpha}^{\dagger} \right] |0\rangle, \quad (2)$$

where $b_i(t)$ is the time-dependent probability amplitude to find the system in the corresponding state i with the initial condition $b_0(0) = 1$ and $b_{\alpha}(0) = 0$. Substitution of Eq. (2) into the time-dependent Schrödinger equation $i\partial_t|\Psi(t)\rangle = H|\Psi(t)\rangle$, leads to an infinite set of coupled linear differential equations for the amplitudes $b(t)$. Applying the Laplace transform

$$\tilde{b}(E) = \int_0^{\infty} b(t) \exp(iEt) dt \quad (3)$$

and taking into account the initial condition, we transform the differential equations for $b(t)$ into an infinite set of algebraic equations for the amplitudes $\tilde{b}(E)$:

$$(E - E_0)\tilde{b}_0(E) - \sum_{\alpha} \Omega_{\alpha} \tilde{b}_{\alpha} = i, \quad (4a)$$

$$(E - E_{\alpha})\tilde{b}_{\alpha}(E) - \Omega_{\alpha} \tilde{b}_0(E) = 0. \quad (4b)$$

In order to solve these equations we replace the amplitude \tilde{b}_{α} in Eq.(4a) by its expression obtained from Eq.(4b). Then we obtain

$$\left[E - E_0 - \sum_{\alpha} \frac{\Omega_{\alpha}^2}{E - E_{\alpha}} \right] \tilde{b}_0(E) = i. \quad (5)$$

Since the states in the reservoir are very dense, one can replace the sum over α by an integral over E_{α} .

$$\sum_{\alpha} \frac{\Omega_{\alpha}^2}{E - E_{\alpha}} = \int \frac{\Omega^2(E_{\alpha})\rho(E_{\alpha})}{E - E_{\alpha}} dE_{\alpha}, \quad (6)$$

where $\rho(E_{\alpha})$ is the density of states in the reservoir. To evaluate this integral, we can split the integral into its principal and singular parts, $-i\delta(E - E_{\alpha})$. (Notice that $E \equiv E + i\epsilon$ in the Laplace transform, Eq. (3)). As a result the original Schrödinger equation (4) is reduced to

$$\left[E - E_0 - \Delta(E) + i\frac{\Gamma(E)}{2} \right] \tilde{b}_0(E) = i, \quad (7a)$$

$$(E - E_{\alpha}) \tilde{b}_{\alpha}(E) - \Omega(E_{\alpha}) \tilde{b}_0(E) = 0, \quad (7b)$$

where $\Gamma(E) = 2\pi\rho(E)\Omega_{\alpha}^2(E)$ and $\Delta(E)$ is the energy-shift due to the principal part of the integral.

Using Eqs. (7) and the inverse Laplace transform one can obtain the occupation probabilities of the levels E_0 and E_{α} [23]. Yet, Eqs. (7) are not convenient if we wish to include the effects of the environment. These effects can be determined in a natural way only in terms of the density matrix. For this reason we transform Eqs. (7) to equations for the density matrix $\sigma_{ij}(t) \equiv b_i(t)b_j^*(t)$. The latter is directly related to the amplitudes $\tilde{b}(E)$ via the inverse Laplace transform

$$\sigma_{ij}(t) = \int_{-\infty}^{+\infty} \frac{dE dE'}{(2\pi)^2} \tilde{b}_i(E) \tilde{b}_j^*(E') e^{i(E' - E)t}. \quad (8)$$

In order to proceed further with our derivations we have to know the E -dependence of Γ and Δ , determined by the density of states $\rho(E_\alpha)$ and the hopping amplitude $\Omega(E_\alpha)$, Eq. (6). We consider below two important cases.

A. Constant width

Let us assume that $\Omega_\alpha^2(E_\alpha)\rho(E_\alpha)$ is weakly dependent on the energy E_α . As a result the width becomes a constant $\Gamma(E) = \Gamma_0$ and the energy shift $\Delta(E)$ tends to zero. In order to transform Eqs. (7) to the equations for the density matrix by using the inverse Laplace transform (8), we multiply each of the Eqs. (7) by the corresponding complex conjugate amplitude $b^*(E')$. For instance by multiplying Eq. (7a) by $b_0^*(E')$ and subtracting the complex conjugated equation multiplied by $b_0(E)$ we obtain

$$(E' - E - i\Gamma_0)\tilde{b}_0(E)\tilde{b}_0^*(E') = -i[\tilde{b}_0(E) + \tilde{b}_0^*(E')], \quad (9)$$

It is quite easy to see that the inverse Laplace transform (8) turns this equation to the following one for the density matrix

$$\dot{\sigma}_{00}(t) = -\Gamma_0\sigma_{00}(t) + [b_0(t) + b_0^*(t)]\delta(t). \quad (10)$$

Notice that the initial time in the inverse Laplace transform (8) corresponds to $t = +0$, which allows us to ignore the term proportional to the δ -function on the right hand side of Eq. (10).

Proceeding in the same way with all the other equations (7), we obtain the following set of equations for the density matrix $\sigma(t)$

$$\dot{\sigma}_{00}(t) = -\Gamma_0\sigma_{00}(t), \quad (11a)$$

$$\dot{\sigma}_{\alpha\alpha}(t) = i\Omega_\alpha(\sigma_{\alpha 0}(t) - \sigma_{0\alpha}(t)) \quad (11b)$$

$$\dot{\sigma}_{\alpha 0}(t) = i\epsilon_{0\alpha}\sigma_{\alpha 0}(t) - i\Omega_\alpha\sigma_{00}(t) - \frac{\Gamma_0}{2}\sigma_{\alpha 0}(t), \quad (11c)$$

with $\epsilon_{0\alpha} = E_0 - E_\alpha$ and $\sigma_{0\alpha} = \sigma_{\alpha 0}^*$.

It is interesting to compare Eqs. (11) with similar Bloch-type equations describing quantum transitions between two isolated levels [24,10]. In the case of the isolated levels (E_1 and E_2), the equations for the density matrix σ are symmetric with respect to E_1 and E_2 . Whereas in the case of transition between the isolated (E_0) and the continuum of states (E_α) the corresponding symmetry, between E_0 and E_α , is broken as can be seen, for example, in the equation for the off-diagonal term $\sigma_{\alpha 0}$ where the coupling with $\sigma_{\alpha\alpha}$ is missing. Eq. (11c).

Solving Eqs. (11) we find the following expressions for the occupation probabilities, σ_{00} and $\sigma_{\alpha\alpha}$, of the levels E_0 and E_α , respectively [23]:

$$\sigma_{00}(t) = e^{-\Gamma_0 t}, \quad (12a)$$

$$\sigma_{\alpha\alpha}(t) = \frac{\Omega_\alpha^2}{(E_\alpha - E_0)^2 + (\Gamma_0/2)^2} \times \left(1 - 2\cos(E_\alpha - E_0)t e^{-\Gamma_0 t/2} + e^{-\Gamma_0 t}\right) \quad (12b)$$

Notice that the line shape, $P(E_\alpha) \equiv \sigma_{\alpha\alpha}(t \rightarrow \infty)\rho$, given by Eq. (12b), is the standard Lorentzian distribution

$$P(E_\alpha) = \frac{\Gamma_0/(2\pi)}{(E_\alpha - E_0)^2 + (\Gamma_0/2)^2} \quad (13)$$

with the width Γ_0 corresponding to the inverse life-time of the quasi-stationary state, Eq. (12a).

B. Lorentzian density of states

Let us consider the same problem studied before but with the decay width Γ in Eq. (7a) dependent on energy. This dependence could be generated either by the density of states in the reservoir $\rho(E_\alpha)$ or by hopping amplitude, Ω_α , depending on E_α . Here, we will restrict our selves to the frequent situation in which the density of states in the reservoir is modulated by a Lorentzian shape, as for instance by the resonant cavity,

$$\rho(E_\alpha) = \bar{\rho} + \frac{\Gamma_1/2\pi}{(E_\alpha - E_1)^2 + \Gamma_1^2/4}. \quad (14)$$

Here $\bar{\rho}$ is a background component and Γ_1 is the width of the Lorentzian centered around E_1 . Substituting Eq. (14) into Eq. (6) and assuming that the hopping amplitude $\Omega(E_\alpha)$ is weakly dependent on the energy E_α , we can easily evaluate the integral (6). Then Eq. (7a) becomes

$$\left(E - E_0 + i\frac{\bar{\Gamma}}{2} - \frac{\Omega_\alpha^2}{E - E_1 + i\Gamma_1/2}\right)\tilde{b}_0(E) = i, \quad (15)$$

with $\bar{\Gamma} = 2\pi\Omega_\alpha^2\bar{\rho}$. Similar to the previous case we transform Eqs. (7) into the rate equations for the corresponding density matrix. For this reason we split Eq. (15) into two coupled equations by introducing an auxiliary amplitude

$$\tilde{b}_1 = \frac{\Omega_\alpha}{E - E_1 + i\Gamma_1/2}\tilde{b}_0. \quad (16)$$

As a result Eqs. (7) become

$$\left(E - E_0 + i\frac{\bar{\Gamma}}{2}\right)\tilde{b}_0(E) - \Omega_\alpha\tilde{b}_1(E) = i \quad (17a)$$

$$\left(E - E_1 + i\frac{\Gamma_1}{2}\right)\tilde{b}_1(E) - \Omega_\alpha\tilde{b}_0(E) = 0 \quad (17b)$$

$$(E - E_\alpha)\tilde{b}_\alpha(E) - \Omega_\alpha\tilde{b}_0(E) = 0 \quad (17c)$$

The amplitude \tilde{b}_1 can be interpreted as the probability amplitude of finding the electron in the state E_1 embedded in the reservoir. Now using the same procedure as that we applied for the derivation of Eqs. (11), we

transform Eqs. (17) into equations for the density matrix $\sigma_{ij}(t)$:

$$\dot{\sigma}_{00}(t) = -\bar{\Gamma}\sigma_{00} + i\Omega_\alpha(\sigma_{01} - \sigma_{10}) \quad (18a)$$

$$\dot{\sigma}_{11}(t) = -\Gamma_1\sigma_{11} + i\Omega_\alpha(\sigma_{10} - \sigma_{01}) \quad (18b)$$

$$\dot{\sigma}_{01}(t) = i\epsilon_{10}\sigma_{01} + i\Omega_\alpha(\sigma_{00} - \sigma_{11}) - \frac{\bar{\Gamma} + \Gamma_1}{2}\sigma_{01} \quad (18c)$$

$$\dot{\sigma}_{\alpha\alpha}(t) = i\Omega_\alpha(\sigma_{\alpha 0} - \sigma_{0\alpha}) \quad (18d)$$

$$\dot{\sigma}_{0\alpha}(t) = i\epsilon_{\alpha 0}\sigma_{0\alpha} + i\Omega_\alpha(\sigma_{00} - \sigma_{1\alpha}) - \frac{\bar{\Gamma}}{2}\sigma_{0\alpha} \quad (18e)$$

$$\dot{\sigma}_{1\alpha}(t) = i\epsilon_{\alpha 1}\sigma_{1\alpha} + i\Omega_\alpha(\sigma_{10} - \sigma_{0\alpha}) - \frac{\Gamma_1}{2}\sigma_{1\alpha}, \quad (18f)$$

where $\epsilon_{ij} = E_i - E_j$ and $\sigma_{ji} = \sigma_{ij}^*$.

Although Eqs. (18) are quite different from Eqs. (11) obtained in the previous case, their interpretation is similar. In fact, Eqs. (18) represent Bloch-type equations describing decay of two-level system, as for instance an electron in the coupled double quantum dots, shown in Fig. 2. (The latter is described by Eqs. (18) for $\bar{\Gamma} = 0$). This is not surprising since the Lorentzian component of the density of states corresponds to a resonance state embedded in the reservoir.

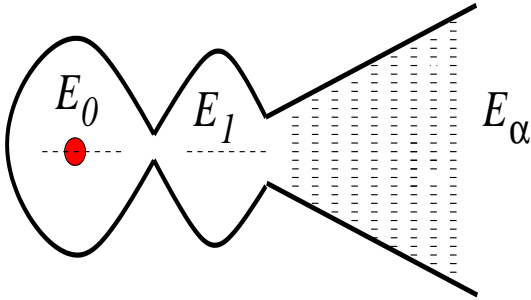


Fig. 2: Double-dot system coupled to the reservoir of continuum states. The electron is initially in the left dot.

Solving Eqs. (18) (or Eqs. (17)) one finds that

$$\sigma_{\alpha\alpha}(t \rightarrow \infty) = \frac{\Omega_\alpha^2 [(E_\alpha - E_1)^2 + \Gamma_1^2/4]}{\left| \left(\epsilon_{\alpha 0} + i\frac{\bar{\Gamma}}{2} \right) \left(\epsilon_{\alpha 1} + i\frac{\Gamma_1}{2} \right) - \Omega_\alpha^2 \right|^2} \quad (19)$$

Thus, the line-shape $P(E_\alpha) \equiv \sigma_{\alpha\alpha}(t \rightarrow \infty)\rho(E_\alpha)$ is not a pure Lorentzian one, in contrast with the previous case, Eq. (13). This is a reflection of non-exponential decay. The latter is generated by the energy dependence of the width $\Gamma(E)$ in Eq. (7a), as for instance in the case of a Lorentzian density of states. Indeed, by solving Eqs. (18a)-(18c) for $\bar{\Gamma} = 0$ we obtain

$$\sigma_{00}(t) = \left| \frac{\Gamma_1 + \omega + 2i\epsilon_{01}}{2\omega} \exp\left(-\frac{\Gamma_1 - \omega}{4}t\right) - \frac{\Gamma_1 - \omega + 2i\epsilon_{01}}{2\omega} \exp\left(-\frac{\Gamma_1 + \omega}{4}t\right) \right|^2, \quad (20)$$

where $\omega = \sqrt{(\Gamma_1 + 2i\epsilon_{01})^2 - 16\Omega_\alpha^2}$. Hence, the decay is not a pure exponential one. In particular, it follows from Eq. (20) that the probability of finding the electron in the initial state for small t is $\sigma_{00}(t) = 1 - \Omega_\alpha^2 t^2$, in contrast with Eq. (12a), describing the exponential decay. Notice, that the absence of linear in t term in $\sigma_{00}(t)$ is a prerequisite for the Zeno effect.

Consider Eq. (20) for $\Gamma_1 \gg \Omega_\alpha, \epsilon_{01}$. One finds that the first exponential in Eq. (20) dominates the behavior of $\sigma_{00}(t)$ when t increases. Thus

$$\sigma_{00}(t) \simeq \exp\left(-\frac{4\Omega_\alpha^2}{\Gamma_1}t\right) \quad \text{for } t \gg 2/\Gamma_1, \quad (21)$$

so that the decay becomes an exponential one. Respectively, the line-shape $P(E_\alpha)$, Eq. (19), becomes Lorentzian in the same limit:

$$P(E_\alpha) \simeq \frac{1}{2\pi} \frac{4\Omega_\alpha^2/\Gamma_1}{(E_\alpha - E_0)^2 + \left(\frac{2\Omega_\alpha^2}{\Gamma_1}\right)^2} \quad (22)$$

Using Eqs. (18a)-(18c) one can also evaluate the averaged decay-time of the electron in the state E_0 , given by

$$T = -\int_0^\infty t \dot{\sigma}_{00}(t) dt = \int_0^\infty \sigma_{00}(t) dt. \quad (23)$$

The last integral can be evaluated directly from Eqs. (18a)-(18c). As a result, we obtain for the decay-time

$$T = \frac{\tau}{1 + \tau\bar{\Gamma}}, \quad (24)$$

where

$$\tau = \frac{1}{\Gamma_1} + \frac{4\epsilon_{10}^2 + (\bar{\Gamma} + \Gamma_1)^2}{4\Omega_\alpha^2(\bar{\Gamma} + \Gamma_1)}. \quad (25)$$

In the case of zero background width, $\bar{\Gamma} = 0$, the electron decay-time is

$$T = \frac{1}{\Gamma_1} + \frac{4(E_1 - E_0)^2 + \Gamma_1^2}{4\Omega_\alpha^2\Gamma_1}. \quad (26)$$

Hence, instead of the intuitively expected answer $1/\Gamma_1$, we find an enhancement of the decay-time. This enhancement can be attributed to an oscillatory behavior of the electron between the states E_0 and E_1 , which does not exist in the previous case of a constant width. In fact, it is even more surprising that for large Γ_1 the electron decay-time T increases with Γ_1 . Indeed, in the limit $\Gamma_1 \gg \Omega_\alpha, \epsilon_{10}$ the decay-time becomes $T \simeq \Gamma_1/4\Omega_\alpha^2$, in accordance with Eqs. (21), (22). Yet, in the opposite limit, $\epsilon_{10} \gg \Gamma_1$, the decay-time is $T \simeq (1 + \epsilon_{10}^2/\Omega_\alpha^2)/\Gamma_1$. Thus it is inversely proportional to Γ_1 , as expected. Such

an unusual behavior of the decay-time can be understood in terms of a broadening of the level E_1 due to its coupling with continuum states E_α , Fig. 2. If $E_0 = E_1$, this broadening results in an effective misalignment of the levels E_0 and E_1 , thus destroying the resonant-tunneling condition. As a result the decay from the level E_0 to continuum slows down. On the other hand, if $E_0 \neq E_1$, the broadening of the level E_1 would effectively diminish the misalignment of the levels $E_{0,1}$, so that the decay would be accelerated.

It has been argued that the slowing down of the decay rate with Γ_1 in two stage processes, as shown in Fig. 2, might be interpreted as the Zeno effect [25]. This would imply that the electron decay from the level E_1 to the states E_α is treated as the measurement of the first transition from the level E_0 to the level E_1 . Such a “measurement” would localize the electron on the level E_0 . Yet, the electron in the reservoir is a part of the same measured system. Strictly speaking, it cannot be considered as an external system to itself. Actually the measurement must always imply an external macroscopic system interacting with the measured electron. Such a measurement device and its quantum mechanical description is provided in the next section.

III. POINT CONTACT AS A DETECTOR OF AN UNSTABLE SYSTEM

As an example of the detector, monitoring decay of an unstable system, we consider a point contact placed near the quantum dot, Fig. 3. The point contact is connected with two separate reservoirs. The reservoirs are filled up to the Fermi levels μ_L and μ_R , respectively. Therefore the current $I = e^2TV/2\pi$ flows from the left (emitter) to the right reservoir (collector), where T is the transmission coefficient of the point contact and $eV = (\mu_L - \mu_R)$ is the bias voltage [26]. (We consider the case of zero temperature). When the dot is occupied, Fig. 3a, the transmission coefficient of the point contact decreases ($T' < T$) due to Coulomb repulsion generated by the electron in the dot. Respectively, the current through the quantum dot diminishes, $I' < I$. However, when the electron is in the reservoir, Fig. 3b, it is far away from the point contact. As a result the transmission coefficient of the point contact becomes again T , and the current increases. Thus, the point contact does represent a detector, which monitors the occupation of the quantum dot. Actually, such a point contact detector has been successfully used in different experiments [27]. Notice that the current variation ($I - I'$) can be a macroscopic quantity if the applied voltage V is large enough.

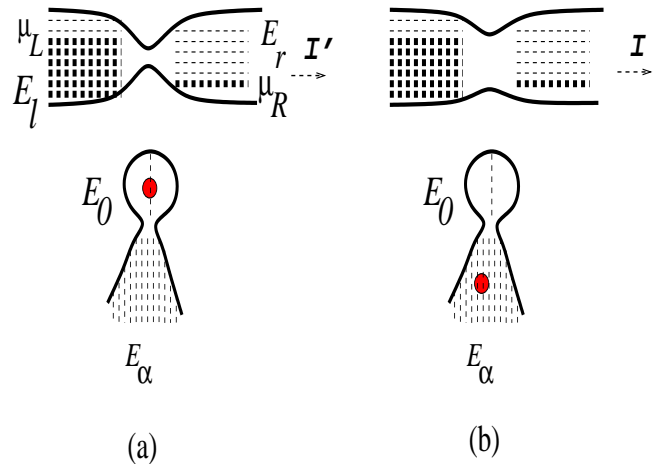


Fig. 3: The point contact detector near the quantum dot. The energy level E_0 of the dot is occupied by an electron (a), which tunnels from the state E_0 , to continuous states E_α of the reservoir (b). μ_L and μ_R are the Fermi levels in the emitter and the collector, respectively.

The dynamics of the entire system is determined by the many-body time-dependent Schrödinger equation $i\partial_t|\Psi(t)\rangle = H|\Psi(t)\rangle$, where the total Hamiltonian consists of three components $H = H_{QD} + H_{PC} + H_{int}$, describing the quantum dot, the point contact detector, and their mutual interaction, respectively. The first component, H_{QD} , is given by Eq. (1). The two additional components, H_{PC} and H_{int} , can also be written in the form of a tunneling Hamiltonian as

$$H_{PC} = \sum_l E_l c_l^\dagger c_l + \sum_r E_r c_r^\dagger c_r + \sum_{l,r} [\Omega_{lr} c_l^\dagger c_r + h.c.]$$

$$H_{int} = \sum_{l,r} [\delta\Omega_{lr} c_l^\dagger c_r + h.c.] c_0^\dagger c_0, \quad (27)$$

where the operators $c_i^\dagger(c_i)$ correspond to the creation (annihilation) of an electron in state i . The Ω_{lr} are the hopping amplitudes between the states E_l , E_r of the point contact. The quantity $\delta\Omega_{lr} = \Omega'_{lr} - \Omega_{lr}$ represents the variation of the point contact hopping amplitude, when the dot is occupied.

Consider now the entire system in the initial condition corresponding to the occupied quantum dot and the reservoirs are filled up to the Fermi levels μ_L and μ_R , Fig. 3a. We denote this state as $|\Psi(0)\rangle = c_0^\dagger|0\rangle$. This state is not stable: the Hamiltonian (2) requires it to decay to continuum states having the form $c_\alpha^\dagger c_i^\dagger c_j^\dagger \dots c_i c_j \dots |0\rangle$. In general, the total wave-function at the time t can be written as

$$|\Psi(t)\rangle = \left[b_0(t) c_0^\dagger + \sum_\alpha b_\alpha(t) c_\alpha^\dagger + \sum_{l,r} b_{lr}(t) c_r^\dagger c_l \right]$$

$$+ \sum_{\alpha, l, r} b_{\alpha l r}(t) c_{\alpha}^{\dagger} c_r^{\dagger} c_l + \dots \Big] |0\rangle. \quad (28)$$

Here $b(t)$ are the probability amplitudes of finding the system in the state defined by the corresponding creation and annihilation operators. As in the previous case, we substitute Eq. (28) into the time dependent Schrödinger equation and use the Laplace transform Eq. (3). Then we find an infinite set of algebraic equations for the amplitudes $\tilde{b}(E)$.

$$(E - E_0)\tilde{b}_0 - \sum_{\alpha} \Omega_{\alpha} \tilde{b}_{\alpha} - \sum_{l, r} \Omega'_{l r} \tilde{b}_{l r} = i, \quad (29a)$$

$$(E - E_{\alpha})\tilde{b}_{\alpha} - \Omega_{\alpha} \tilde{b}_0 - \sum_{l, r} \Omega_{l r} \tilde{b}_{\alpha l r} = 0, \quad (29b)$$

$$(E + E_l - E_r)\tilde{b}_{l r} - \sum_{\alpha} \Omega_{\alpha} \tilde{b}_{\alpha l r} - \Omega'_{l r} \tilde{b}_0 - \sum_{l', r'} \Omega'_{l' r'} \tilde{b}_{l l' r r'} = 0 \quad (29c)$$

.....

These equations look much more complicated than the previous ones in Eqs. (7), describing the one-particle decay. Nevertheless, they can also be transformed into Bloch-type rate equations by tracing over the continuous degrees of freedom. Such a technique has been derived in [10,14,28]. In this paper we extend this technique by converting Eqs. (29) into the rate equations, even without tracing over all continuum states [12]. As a results we obtain generalized Bloch-type equations that determine the energy distribution of the tunneling particles in the reservoirs, as well as the time-development of the entire system.

As in the previous case of the one-electron decay we replace the sums in Eqs. (29) by the integrals, $\sum_k \rightarrow \int \rho(E_k) dE_k$. Consider first the terms related to the left and the right reservoirs of the detector, Fig. 3. Let us assume that the corresponding hopping amplitudes, $\Omega_{l r}$, and the density of states $\rho(E_{l, r})$ are weakly dependent on the energies: $\Omega_{l r} \equiv \Omega(E_l, E_r) = \Omega$, and $\rho(E_{l, r}) = \rho_{L, R}$. Let us also assume the large bias limit, $eV \gg \Omega^2 \rho_{L, R}$, so the integration limits can be extended to infinity. Then the integrations can be treated analytically. Indeed, consider for instance Eq. (29a). Replacing the amplitude $\tilde{b}_{l r}$ by the corresponding expression obtained from Eq. (29c), we find

$$\left(E - E_0 - \int \frac{\Omega'^2 \rho_L \rho_R dE_l dE_r}{E + E_l - E_r} \right) \tilde{b}_0(E) - \sum_{\alpha} \Omega_{\alpha} \tilde{b}_{\alpha} + \mathcal{F} = i, \quad (30)$$

where \mathcal{F} denotes the other terms where the amplitudes \tilde{b}_0 cannot be factorized out the integral. The integral

in Eq. (30) is treated in the same way as in Eq. (6) for one-electron tunneling. Namely, we split the integral into its principle value and singular part. The singular part yields $iD'/2$, where $D' = 2\pi\Omega'^2 \rho_L \rho_R eV = eTV/(2\pi)$ [29], and the principal part is zero.

Consider now the non-factorizable terms \mathcal{F} in Eq. (30). These terms vanish in the large bias limit. Indeed, all the singularities of the amplitude $\tilde{b}(E, E_l, E_{l'}, E_r, E_{r'})$ in the $E_l, E_{l'}$ -variables lie below the real axis. This can be seen directly from Eqs. (29) by noting that E lies above the real axis in the Laplace transform Eq. (3). Assuming that the transition amplitudes Ω as well as the density of states $\rho_{L, R}$ are independent of $E_{l, r}$, one can close the integration contour in the upper $E_{l, r}$ -plane. Since the integrand decreases faster than $1/E_{l, r}$, the resulting integral is zero.

Applying analogous considerations to the other equations of the system (29), we arrive at the following set of equations [10,14]

$$\left(E - E_0 + i\frac{D'}{2} \right) \tilde{b}_0 - \sum_{\alpha} \Omega_{\alpha} \tilde{b}_{\alpha} = i, \quad (31a)$$

$$\left(E - E_{\alpha} + i\frac{D}{2} \right) \tilde{b}_{\alpha} - \Omega_{\alpha} \tilde{b}_0 = 0, \quad (31b)$$

$$\left(E + E_l - E_r + i\frac{D'}{2} \right) \tilde{b}_{l r} - \Omega' \tilde{b}_0 - \sum_{\alpha} \Omega_{\alpha} \tilde{b}_{\alpha l r} = 0, \quad (31c)$$

.....

where $D = (2\pi)|\Omega_{l r}|^2 \rho_L \rho_R (\mu_l - \mu_r) = eTV/(2\pi)$.

Proceeding in the same way with the remaining sum over the states E_{α} we finally arrive to the equations

$$\left(E - E_0 + i\frac{D'}{2} - \mathcal{I}(E) \right) \tilde{b}_0 = i, \quad (32a)$$

$$\left(E - E_{\alpha} + i\frac{D}{2} \right) \tilde{b}_{\alpha} - \Omega_{\alpha} \tilde{b}_0 = 0, \quad (32b)$$

$$\left(E + \epsilon_{l r} + i\frac{D'}{2} - \mathcal{I}(E - \epsilon_{l r}) \right) \tilde{b}_{l r} - \Omega' \tilde{b}_0 = 0, \quad (32c)$$

.....

where $\epsilon_{l r} = E_l - E_r$ and

$$\mathcal{I}(E) \equiv \Delta(E) - i\frac{\Gamma(E)}{2} = \int \frac{\Omega_{\alpha}^2(E_{\alpha}) \rho(E_{\alpha})}{E - E_{\alpha} + iD/2} dE_{\alpha}, \quad (33)$$

Let us introduce the reduced density matrix of the entire system that includes the measured electron and the detector:

$$\sigma_{i, j}^{(n, n')}(t) = \langle \Psi(t) | n', j \rangle \langle n, i | \Psi(t) \rangle, \quad (34)$$

where $|n, i\rangle$ denotes the state with n electrons in the right reservoir, i.e. $\sum_r c_r^{\dagger} c_r |n\rangle = n|n\rangle$, and $i, j = \{0, \alpha\}$ denotes the state of the observed electron. This density

matrix can be directly related to the amplitudes $b(t)$ of Eq. (28):

$$\begin{aligned} \sigma_{00}^{(0,0)}(t) &= |b_0(t)|^2, & \sigma_{00}^{(0,1)}(t) &= \sum_{l,r} |b_0(t)b_{lr}^*(t)|^2, \\ \sigma_{00}^{(1,1)}(t) &= \sum_{l,r} |b_{lr}(t)|^2, & \sigma_{0\alpha}^{(0,1)}(t) &= \sum_{l,r,\alpha} |b_0(t)b_{\alpha lr}^*(t)|^2, \\ &\dots\dots & &\dots\dots \end{aligned} \quad (35)$$

Now we transform Eqs. (32) into equations for the density matrix $\sigma_{i,j}^{(n,n')}(t)$, without their explicit solution. It can be done by using the same procedure as in Sect. 2, for two cases, corresponding to weak and Lorentzian energy dependence of the function $\mathcal{I}(E)$, Eq. (33). Since we take for the definiteness the amplitude Ω_α as independent of E_α , these two cases correspond to constant or Lorentzian density of states $\rho(E_\alpha)$ in the reservoir. We demonstrate below that the influence of the measurement of the decay is distinctly different in both cases.

A. Constant density of states

If the product $\Omega_\alpha^2 \rho(E_\alpha)$ in Eq. (33) is weakly dependent on the energy E_α , one can replace $\Gamma(E) = \Gamma_0$, and $\Delta(E) = 0$ in Eqs. (32)-(33), where $\Gamma_0 = 2\pi\Omega_\alpha^2\rho = \text{const}$. In order to convert Eqs. (32) into equations for the density matrix, we multiply each of these equations by the corresponding complex conjugate amplitude $b^*(E')$ and subtract the complex conjugated equation multiplied by $b_\alpha(E)$. For instance Eq. (32b) becomes

$$\begin{aligned} (E - E' + iD)b_\alpha(E)b_\alpha^*(E') \\ = \Omega_\alpha[b_0(E)b_\alpha^*(E') - b_0^*(E')b_\alpha(E)] \end{aligned} \quad (36)$$

Then the inverse Laplace transform, Eq. (8), converts Eq. (36) to the following equation for the density matrix

$$\dot{\sigma}_{\alpha\alpha}^{(0,0)}(t) = -D\sigma_{\alpha\alpha}^{(0,0)}(t) + i\Omega_\alpha[\sigma_{\alpha 0}^{(0,0)}(t) - \sigma_{0\alpha}^{(0,0)}(t)]. \quad (37)$$

Proceeding in the same way with all other equations (32) and integrating over the continuum states of the collector and the emitter, we obtain the following infinite set of equations for the density matrix $\sigma(t)$

$$\dot{\sigma}_{00}^{(n)} = -(\Gamma_0 + D')\sigma_{00}^{(n)} + D'\sigma_{00}^{(n-1)} \quad (38a)$$

$$\dot{\sigma}_{\alpha\alpha}^{(n)} = -D\sigma_{\alpha\alpha}^{(n)} + D\sigma_{\alpha\alpha}^{(n-1)} + i\Omega_\alpha(\sigma_{0\alpha}^{(n)} - \sigma_{\alpha 0}^{(n)}) \quad (38b)$$

$$\begin{aligned} \dot{\sigma}_{\alpha 0}^{(n)} &= i(E_0 - E_\alpha)\sigma_{\alpha 0}^{(n)} - i\Omega_\alpha\sigma_{00}^{(n)} \\ &\quad - \frac{\Gamma_0 + D + D'}{2}\sigma_{\alpha 0}^{(n)} + \sqrt{DD'}\sigma_{\alpha 0}^{(n-1)}. \end{aligned} \quad (38c)$$

Here we denoted $\sigma_{\alpha 0}^{(n)} \equiv \sigma_{\alpha 0}^{(n,n)}$. The initial conditions correspond to $\sigma_{ij}^{(n,n')}(0) = \delta_{i0}\delta_{j0}\delta_{n0}\delta_{n'0}$. Notice, that Eqs. (38) involves only the diagonal density matrix elements with respect of the number of electrons in the

collector n . This, however, does not imply the vanishing of the off-diagonal terms, $\sigma^{(n,n')}$. It means only their decoupling from the diagonal terms in the equations of motion. This always takes place, in transition between continuous states [14,28].

Eqs. (38) represent a generalization of the previously derived Bloch-type equations for quantum transport in mesoscopic systems [10,14]. They have clear physical interpretation. Consider for instance Eq. (38a) for the probability of finding the electron inside the dot and n electrons in the collector. This state decays due to one-electron hopping to the collector (with the rate D'), or due to the electron tunneling out of the dot (with the rate Γ_0). These processes are described by the first (“loss”) term in Eq. (38a). On the other hand, there exists the opposite (“gain”) process when the state with $(n-1)$ electrons in the collector converts into the state with n electrons in the collector. It also takes place due to penetration of one electron through the point contact with the same rate D' . This process is described by the second term in Eq. (38a).

The evolution of the off-diagonal density matrix elements $\sigma_{\alpha 0}^{(n)}(t)$ is given by Eq. (38c). It can be interpreted in the same way as the rate equation for the diagonal terms. Notice, however, the difference between the “loss” and the “gain” terms. The latter can appear only due to coherent transition of the whole linear superposition [10,14,28].

In order to determine the time-evolution of the observed electron we have to trace out over the detector states n in Eqs. (38). As a result we obtain the following rate equations for the reduced density matrix $\sigma(t) \equiv \sum_n \sigma^{(n)}(t)$:

$$\dot{\sigma}_{00} = -\Gamma_0\sigma_{00} \quad (39a)$$

$$\dot{\sigma}_{\alpha\alpha} = i\Omega_\alpha(\sigma_{\alpha 0} - \sigma_{0\alpha}) \quad (39b)$$

$$\dot{\sigma}_{\alpha 0} = i(E_0 - E_\alpha)\sigma_{\alpha 0} - i\Omega_\alpha\sigma_{00} - \frac{\Gamma_0 + \Gamma_d}{2}\sigma_{\alpha 0}. \quad (39c)$$

Here $\Gamma_d = (\sqrt{D} - \sqrt{D'})^2$ is the decoherence rate, generated by the detector [10].

Let us compare these equations with Eqs. (11), describing decay of a single electron, which is not observed by the outside detector. We find the difference only in equations for the off-diagonal term, Eqs. (11c) and (39c), respectively. The interaction with the detector results in an increase of the damping term. All other equations are unaffected by the measurement. As a result, the probability of finding the system undecayed remains the same as in the previous case, $\sigma_{00}(t) = \exp(-\Gamma_0 t)$. It means that the continuous monitoring of the unstable system does not slow down its decay rate. Nevertheless, it affects the energy distribution of the tunneling electron $P(E_\alpha) \equiv \sigma_{\alpha\alpha}(t \rightarrow \infty)\rho$. Indeed, by solving Eqs. (39) in the limit of $t \rightarrow \infty$ we find a Lorentzian centered about $E_\alpha = E_0$:

$$P(E_\alpha) = \frac{(\Gamma_0 + \Gamma_d)/2\pi}{(E_0 - E_\alpha)^2 + (\Gamma_0 + \Gamma_d)^2/4}. \quad (40)$$

If there is no coupling with the detector, $\Gamma_d = 0$, the Lorentzian width (the line-width) Γ_0 is the inverse lifetime of the quasi-stationary state, as given by Eq. (13). However, as follows from Eq. (40), the measurement results in a broadening of the line-width due to the decoherence generated by the detector. It now becomes $\Gamma_0 + \Gamma_d$.

On the first sight this result might look surprising. Indeed, it is commonly accepted that the line-width does correspond to the life-time. Yet, we demonstrated here that it might not be the case, when the system interacts with an environment (the detector). To understand this result, one might think of the following argument. Due to the measurement, the energy level E_0 suffers an additional broadening of the order of Γ_d . However, this broadening does not affect the decay rate of the electron Γ_0 , since the exact value of E_0 relative to E_α is irrelevant to the decay process. In contrast, the probability distribution $P(E_\alpha)$ is affected because it does depend on the position of E_0 relative to E_α as it can be seen in Eq. (40).

Although our result has been proved for a specific detector, we expect it to be valid for the general case, provided that the density of states ρ and the transition amplitude Ω_α for the observed electron vary slowly with energy. This condition is sufficient to obtain a pure exponential decay of the state E_0 . On the contrary, if the product $\Omega_\alpha^2 \rho(E_\alpha)$ depends sharply on energy E_α , it yields strong E -dependence of Γ and Δ in Eqs. (7), (32). This modifies both the exponential dependence of the decay probability, $\sigma_{00}(t)$, and the energy distribution, $P(E_\alpha)$, as that given by Eqs. (19) and (20). In particular, the decay probability for the small t would be proportional to t^2 . Therefore it is important to investigate the influence of the measurement in this case.

B. Lorentzian density of states

Consider for the definiteness that the density of states $\rho(E_\alpha)$ of the Lorentzian form, given by Eq. (14) and the amplitude Ω_α is slowly dependent on the energy E_α . In this case one obtains from Eq. (33)

$$\Delta(E) - i\frac{\Gamma(E)}{2} = -i\frac{\bar{\Gamma}}{2} + \frac{\Omega_\alpha^2}{E - E_1 + i(D + \Gamma_1)/2}. \quad (41)$$

Substituting this result into Eqs. (32) and introducing the auxiliary amplitudes

$$\tilde{b}_1 = \frac{\Omega_\alpha}{E - E_1 + i(D + \Gamma_1)/2} \tilde{b}_0 \quad (42a)$$

$$\tilde{b}_{1lr} = \frac{\Omega_\alpha}{E + E_l - E_r - E_1 + i(D + \Gamma_1)/2} \tilde{b}_{lr} \quad (42b)$$

$$\dots \quad (42c)$$

we can rewrite Eqs. (32) in the following form

$$\left(E - E_0 + i\frac{D' + \bar{\Gamma}}{2}\right) \tilde{b}_0 - \Omega_\alpha \tilde{b}_1 = i, \quad (43a)$$

$$\left(E - E_1 + i\frac{D + \Gamma_1}{2}\right) \tilde{b}_1 - \Omega_\alpha \tilde{b}_0 = 0 \quad (43b)$$

$$\left(E - E_\alpha + i\frac{D}{2}\right) \tilde{b}_\alpha - \Omega_\alpha \tilde{b}_0 = 0, \quad (43c)$$

$$\left(E + E_l - E_r + i\frac{D' + \bar{\Gamma}}{2}\right) \tilde{b}_{lr} - \Omega' \tilde{b}_{1lr} = 0, \quad (43d)$$

.....

where $\bar{\Gamma} = 2\pi\Omega_\alpha^2\rho$. The amplitudes $b_1(t)$, $b_{1lr}(t)$, ... are the probability amplitudes of finding the electron on the resonant level E_1 of the continuum, for different numbers of electrons in the collector.

It is quite clear that Eqs. (43) describe an unstable two-level system, which is continuously monitored by the point contact detector. If $\bar{\Gamma} = 0$ the entire system is equivalent to that shown in Fig. 4, where the penetrability of the point contact is affected only when the observed electron occupies the level E_0 .

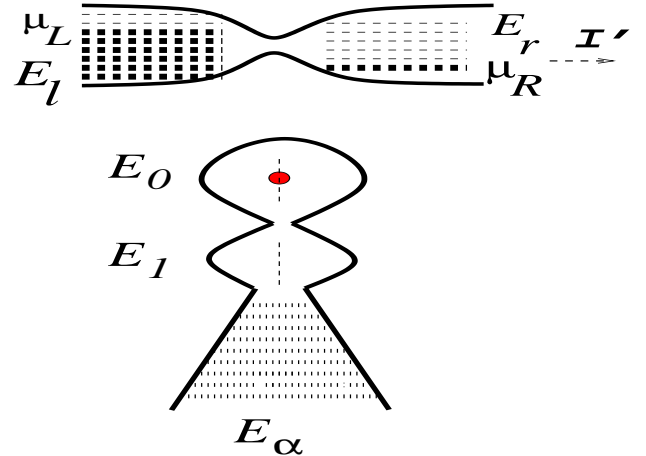


Fig. 4: The point contact detector near the double-dot. The energy level E_0 of the first dot is initially occupied by an electron.

Using the same procedure as in the previous case we transform Eqs. (43) into equations for the density matrix $\sigma(t)$. Finally we obtain the following set of equations, which involves only the diagonal terms in n (similar to Eqs. (38)). For simplicity we consider only the case of $\bar{\Gamma} = 0$.

$$\dot{\sigma}_{00}^{(n)} = -D'\sigma_{00}^{(n)} + D'\sigma_{00}^{(n-1)} + i\Omega_\alpha(\sigma_{01}^{(n)} - \sigma_{10}^{(n)}) \quad (44a)$$

$$\dot{\sigma}_{11}^{(n)} = -(D + \Gamma_1)\sigma_{11}^{(n)} + D\sigma_{11}^{(n-1)} + i\Omega_\alpha(\sigma_{10}^{(n)} - \sigma_{01}^{(n)}) \quad (44b)$$

$$\dot{\sigma}_{01}^{(n)} = i\epsilon_{10}\sigma_{01} + i\Omega_\alpha(\sigma_{00}^{(n)} - \sigma_{11}^{(n)})$$

$$-\frac{D+D'+\Gamma_1}{2}\sigma_{01}^{(n)} + \sqrt{DD'}\sigma_{01}^{(n-1)} \quad (44c)$$

$$\dot{\sigma}_{\alpha\alpha}^{(n)} = -D\sigma_{\alpha\alpha}^{(n)} + D\sigma_{\alpha\alpha}^{(n-1)} + i\Omega_\alpha(\sigma_{\alpha 1}^{(n)} - \sigma_{1\alpha}^{(n)}) \quad (44d)$$

$$\begin{aligned} \dot{\sigma}_{0\alpha}^{(n)} &= i\epsilon_{\alpha 0}\sigma_{0\alpha}^{(n)} + i\Omega_\alpha(\sigma_{00}^{(n)} - \sigma_{1\alpha}^{(n)}) \\ &\quad - \frac{D+D'}{2}\sigma_{0\alpha}^{(n)} + \sqrt{DD'}\sigma_{0\alpha}^{(n-1)} \end{aligned} \quad (44e)$$

$$\begin{aligned} \dot{\sigma}_{1\alpha}^{(n)} &= i\epsilon_{\alpha 1}\sigma_{1\alpha}^{(n)} + i\Omega_\alpha(\sigma_{10}^{(n)} - \sigma_{0\alpha}^{(n)}) \\ &\quad - \frac{2D+\Gamma_1}{2}\sigma_{1\alpha}^{(n)} + D\sigma_{1\alpha}^{(n-1)}. \end{aligned} \quad (44f)$$

These equations describe the microscopic behavior of the measured system and the detector at once. Their physical meaning is similar to that given for Eqs. (38). In order to find the time-evolution of the observed electron alone we trace out over the detector states n in Eq. (44). As a result, we obtain the following equations describing the time evolution of the corresponding reduced density matrix elements

$$\dot{\sigma}_{00} = i\Omega_\alpha(\sigma_{01} - \sigma_{10}) \quad (45a)$$

$$\dot{\sigma}_{11} = -\Gamma_1\sigma_{11} + i\Omega_\alpha(\sigma_{10} - \sigma_{01}) \quad (45b)$$

$$\dot{\sigma}_{01} = i\epsilon_{10}\sigma_{01} + i\Omega_\alpha(\sigma_{00} - \sigma_{11}) - \frac{\Gamma_1 + \Gamma_d}{2}\sigma_{01} \quad (45c)$$

$$\dot{\sigma}_{\alpha\alpha} = i\Omega_\alpha(\sigma_{\alpha 0} - \sigma_{0\alpha}) \quad (45d)$$

$$\dot{\sigma}_{0\alpha} = i\epsilon_{\alpha 0}\sigma_{0\alpha} + i\Omega_\alpha(\sigma_{00} - \sigma_{1\alpha}) - \frac{\Gamma_d}{2}\sigma_{0\alpha} \quad (45e)$$

$$\dot{\sigma}_{1\alpha} = i\epsilon_{\alpha 1}\sigma_{1\alpha} + i\Omega_\alpha(\sigma_{10} - \sigma_{0\alpha}) - \frac{\Gamma_1}{2}\sigma_{1\alpha}, \quad (45f)$$

where $\Gamma_d = (\sqrt{D} - \sqrt{D'})^2$ is the decoherence rate, generated by the detector. At first sight Eqs. (45) resemble Eqs. (18), where the background width $\bar{\Gamma}$ is replaced by the decoherence width Γ_d generated by the detector. Yet, Γ_d does not enter the equations for diagonal density matrix elements, in contrast with the background width $\bar{\Gamma}$ that appears in Eq. (18b). This very essential difference follows from the fact that the measurement is a non-invasive one, and therefore it does not result in additional dissipation processes.

Eqs. (45) give a comprehensive description of the measured system under continuous monitoring, including its energy distribution in the continuum, $P(E_\alpha) \equiv \sigma_{\alpha\alpha}(t \rightarrow \infty)\rho(E_\alpha)$. The latter can be obtained from Eqs. (45) without their explicit solution. Indeed, let us integrate each of Eqs. (45) in the interval $0 \leq t < \infty$ and take into account the initial condition $\sigma_{00}(0) = 1$, $\sigma_{ij}(0) = 0$ and $\sigma_{ij}(\infty) = 0$, except for $\sigma_{\alpha\alpha}(\infty) \neq 0$. Then we obtain the following algebraic equations for $\bar{\sigma} = \int_0^\infty \sigma(t)dt$:

$$i\Omega_\alpha(\bar{\sigma}_{01} - \bar{\sigma}_{10}) = -1 \quad (46a)$$

$$-\Gamma_1\bar{\sigma}_{11} + i\Omega_\alpha(\bar{\sigma}_{10} - \bar{\sigma}_{01}) = 0 \quad (46b)$$

$$i\epsilon_{10}\bar{\sigma}_{01} + i\Omega_\alpha(\bar{\sigma}_{00} - \bar{\sigma}_{11}) - \frac{\Gamma_1 + \Gamma_d}{2}\bar{\sigma}_{01} = 0 \quad (46c)$$

$$i\epsilon_{\alpha 0}\bar{\sigma}_{0\alpha} + i\Omega_\alpha(\bar{\sigma}_{00} - \bar{\sigma}_{1\alpha}) - \frac{\Gamma_d}{2}\bar{\sigma}_{0\alpha} = 0 \quad (46d)$$

$$i\epsilon_{\alpha 1}\bar{\sigma}_{1\alpha} + i\Omega_\alpha(\bar{\sigma}_{10} - \bar{\sigma}_{0\alpha}) - \frac{\Gamma_1}{2}\bar{\sigma}_{1\alpha} = 0, \quad (46e)$$

where $\bar{\sigma}_{ji} = \bar{\sigma}_{ij}^*$. The energy distribution is $\sigma_{\alpha\alpha}(\infty)\rho(E_\alpha) = 2\Omega_\alpha \text{Im}\bar{\sigma}_{0\alpha}\rho(E_\alpha)$.

IV. ZENO AND ANTI-ZENO EFFECT

In order to determine how the measurement affects the measured system, we solve Eqs. (45), (46) for $\Gamma_d \neq 0$ and compare the solution with the corresponding one, obtained for $\Gamma_d = 0$. Let us consider $\Gamma_1 \gg \Omega_\alpha$, where the system displays an exponential decay, Eq. (21), for large enough t .

Let us first examine the probability of finding the system undecayed, $\sigma_{00}(t)$, given by Eqs. (45a)-(45c). This quantity as a function of time (in the units Ω_α^{-1}) is shown in Fig. 5 in the logarithmic scale for $\Gamma_1/\Omega_\alpha = 10$ and (a): $\epsilon_{10} = E_1 - E_0 = 0$, (b): $\epsilon_{10} = 10\Omega_\alpha$.

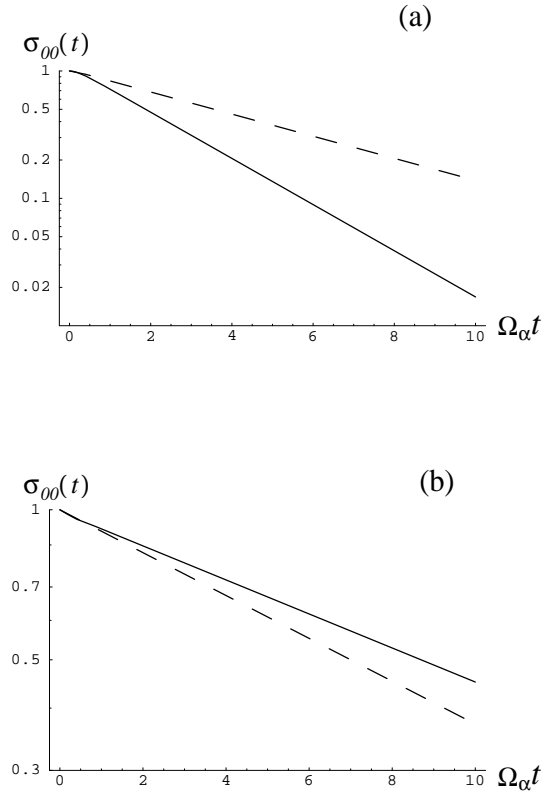


Fig. 5: The probability of finding the electron inside the quantum dot at the level E_0 (Fig. 4), where (a): $E_0 = E_1$, and (b): $E_1 - E_0 = 10\Omega_\alpha$. The solid line corresponds to $\Gamma_d = 0$ (no measurement) and the dashed line to $\Gamma_d = 10\Omega_\alpha$.

One finds from Fig. 5a that decay rate of the electron monitored by the detector (the dashed line) slows down, as expected from the Zeno effect. Yet, if the levels E_0 and E_1 are not aligned, the situation is different. It follows from Fig. 5b that the continuous monitoring of the decayed system leads to an acceleration of the decay, just the opposite to what is expected from Zeno effect (the anti-Zeno effect [30]). However, the later does not take place at very short times, where the continuous observation still slows down the decay rate. This can be seen clearly in Fig. 6, which magnifies the small t -region ($t < \Omega_\alpha^{-1}$) of Fig. 5b.

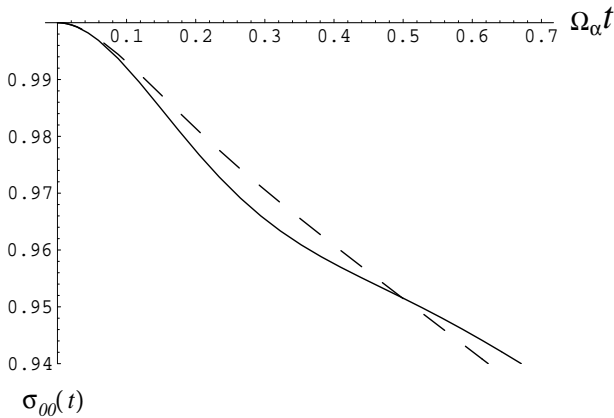


Fig. 6: The probability of finding the electron undecayed for small t , and $(E_1 - E_0) = 10\Omega_\alpha$. All parameters are the same as in Fig. 5b.

Actually, the Zeno and anti-Zeno effects can be revealed from the analytical solution of Eqs. (45a)-(45c) for $t \gg \Omega_\alpha^{-1}$. Indeed, the behavior of $\sigma_{00}(t)$ in this region is dominated by the exponent with lesser exponential factor. The latter can be found directly from the secular determinant of Eqs. (45a)-(45c) (and $\sigma_{10} = \sigma_{01}^*$) in the limit of $\Gamma_1 \gg \Omega_\alpha$. In which case one obtains

$$\sigma_{00}(t) \simeq \exp\left(-\frac{4(\Gamma_1 + \Gamma_d)\Omega_\alpha^2}{4\epsilon_{\alpha 0}^2 + (\Gamma_1 + \Gamma_d)^2}t\right) \quad (47)$$

Therefore if $\epsilon_{01} \ll \Gamma_1 + \Gamma_d$, the second term in the denominator of Eq. (47) dominates. As a result, the decay rate slows down with the decoherence rate Γ_d (Zeno effect). On the other hand, if $\epsilon_{01} \gg \Gamma_1 + \Gamma_d$, the first term dominates in the denominator of Eq. (47) and the decay accelerates with Γ_d (anti-Zeno effect).

One can arrive to the same conclusion by evaluating the average decay-time T of the electron in the state E_0 , Eq. (23). This can be obtained directly from Eqs. (45a)-(45c). In fact we find

$$T = \frac{1}{\Gamma_1} + \frac{4\epsilon_{01}^2 + (\Gamma_1 + \Gamma_d)^2}{4\Omega_\alpha^2(\Gamma_1 + \Gamma_d)}. \quad (48)$$

This is precisely the inverse exponential factor of Eq. (47) in the limit of $\Gamma_1 \gg \Omega_\alpha$.

Consider now the energy distribution of the tunneling electron in the reservoir, $P(E_\alpha) = \sigma_{\alpha\alpha}(\infty)\rho(E_\alpha)$, given by Eqs. (46). In the case of aligned levels, $\epsilon_{01} = 0$, one finds:

$$P(E_\alpha) = \frac{2(\Gamma_1 + \Gamma_d)(\Gamma_1\Gamma_d + 4\Omega_\alpha^2)/\pi}{16\epsilon_{\alpha 0}^4 + 4\epsilon_{\alpha 0}^2(\Gamma_1^2 + \Gamma_d^2 - 8\Omega_\alpha^2) + (\Gamma_1\Gamma_d + 4\Omega_\alpha^2)^2} \quad (49)$$

If $\epsilon_{01} \neq 0$, the analytical expression for $P(E_\alpha)$ is more complicated and less transparent. Therefore it is not presented here.

It follows from Eq. (49) that the width of the energy distribution does not correspond anymore to the inverse decay time, given by Eqs. (47), (48). This stays in contrast with Eq. (22), where the line-width is precisely the inverse decay-time. Moreover the width of the energy distribution, given by Eq. (49) always increases with the decoherence rate Γ_d , although the corresponding inverse decay-time decreases with Γ_d , Eqs. (47), (48). Such a broadening of the energy distribution is shown explicitly in Fig. 7 that displays $P(E_\alpha)$, Eq. (49), for $\Gamma_d = 0$ (the solid line) and $\Gamma_d = 10\Omega_\alpha$ (the dashed line). Fig. 7 shows

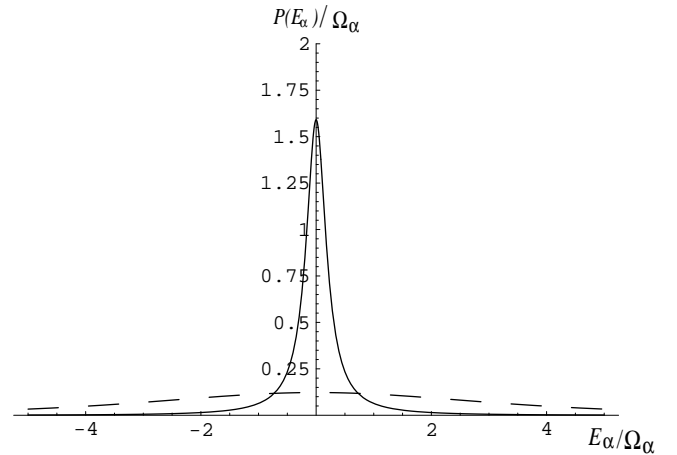


Fig. 7: The energy distribution of the tunneling electron, $P(E_\alpha)$ for $E_1 = E_0$, and $\Gamma_1 = 10\Omega_\alpha$. The solid line correspond to $\Gamma_d = 0$ and the dashed line to $\Gamma_d = \Gamma_1$.

that the width of the energy distribution increases very strongly with Γ_d , so that $P(E_\alpha)$ is almost flat for $\Gamma_d \gg \Omega_\alpha$. In fact, the same strong broadening of the energy distribution takes place for $E_0 \neq E_1$.

The described above measurement effects can be partially interpreted in terms of broadening of the level E_0 induced by the detector. One can expect that this broadening would always lead to spreading of the energy distribution. On the other hand, its influence on the decay rate depends whether the levels E_0 and E_1 are aligned or not. If $E_0 = E_1$ the broadening of the level E_0 destroys the resonant-tunneling condition, so that the decay to continuum slows down. However, if $E_0 \neq E_1$, the same broadening would effectively diminish the levels displacement. As a result, the decay rate should increase. Yet, these arguments are not working at very short times, when the decay rate slows down even for $E_0 \neq E_1$, as shown in Fig. 6.

In general, such intuitive arguments, based only on the level broadening cannot explain all features of the energy distribution $P(E_\alpha)$, especially if the coupling of the level E_1 with the reservoir is weak. In this case the energy distribution, given by Eqs. (46) shows rather unusual dependence on the decoherence rate, Γ_d , generated by the detector. Let us take, for instance, $E_0 = 0$, $E_1 = 5\Omega_\alpha$ and $\Gamma_1 = 0.5\Omega_\alpha$. The corresponding energy distribution $P(E_\alpha)$ is shown in Fig. 8 for $\Gamma_d = 0$ (the solid line), $\Gamma_d = 0.5\Omega_\alpha$ (the dashed line) and $\Gamma_d = 10\Omega_\alpha$ (the dashed-dot line).

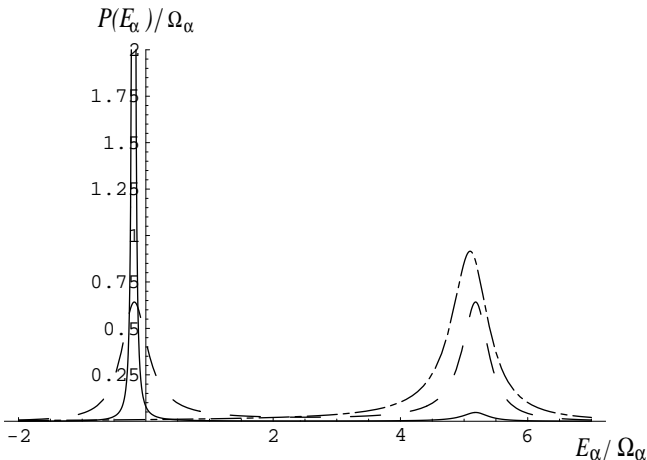


Fig. 8: The energy distribution $P(E_\alpha)$ as given by Eq. (46) for $E_0 = 0$, $E_1 = 5\Omega_\alpha$, and $\Gamma_1 = 0.5\Omega_\alpha$. The solid line correspond to $\Gamma_d = 0$ the dashed line to $\Gamma_d = 0.5\Omega_\alpha$, and the dashed-dot line to $\Gamma_d = 10\Omega_\alpha$.

If there is no measurement ($\Gamma_d = 0$) the energy dis-

tribution $P(E_\alpha)$ is strongly peaked near E_0 , whereas the second peak, at $E_\alpha \simeq E_1$, is almost invisible. Yet, by switching the detector on, the second peak increases with Γ_d . In fact, both peaks are equally pronounced already for $\Gamma_d = \Gamma_1$. Then, for $\Gamma_d = 20\Gamma_1$ the second peak becomes a dominant one (the dashed-dot line), whereas the first peak practically disappears.

Thus we found that continuous monitoring of an electron in a double-dot system, weakly coupled with a reservoir changes completely the intensity of spectral lines. This can be partially interpreted in the following way. Consider first the case of no measurement, $\Gamma_d = 0$. Then a small coupling with the reservoir (Γ_1) cannot essentially affect the eigenstates of the system. These are close to $E_{0,1}$, providing that these levels are strongly detuned. Therefore the peak in the energy distribution of the tunneling electron lies near E_0 , since the electron occupies this level. However, if we switch on the detector, it would decohere the electron inside the double-dot, before it tunnels to the reservoir. This means that electron tends to be equally distributed between the dots. Yet the second dot is directly coupled with the reservoir, whereas the first dot is not, (Fig. 4). As a result, the energy distribution would display the peak near E_1 .

V. SUMMARY

We presented detailed quantum-mechanical analyses of a decayed quantum system under continuous monitoring. As an example we considered an electron tunneling from a discrete level of quantum dot to the empty reservoir. The essential point in our analysis is a full quantum mechanical account of the macroscopic (mesoscopic) detector. This allowed us to investigate quantum Zeno effect as generated by the Schrödinger evolution of the entire system, without invoking the projection postulate. In contrast with the previous treatments, which concentrate only on the time-evolution, we analyzed here the complementary energy distribution of the decayed system, as well.

The results of our analysis clearly demonstrate that the evolution of a decayed system under continuous monitoring is crucially related to the energy dependence of the density of states in the reservoir and the tunneling amplitude. If these quantities are weakly dependent on the energy, a pure exponential decay of the quantum system takes place. In this case the measurement does not affect the decay rate. Yet, the energy distribution of the electron in the reservoir becomes strongly broadened. As a result, the corresponding line-width is no more given by the inverse decay time.

In the case of strong energy dependence of the density of states (or of the tunneling amplitude) the situation is different. As an example we considered the Lorentzian component in the density of states of the width greater

than the tunneling amplitude. In this case the decay is not an exponential one for small times. But it becomes exponential when the time increases. Nevertheless, in contrast with the previous case the measurement affects the decay rate, even in the exponential regime. The effect, however, depends on displacement between the initial state energy and the mid-energy of the Lorentzian density of states. If these energies are close to each other, we obtain the expected Zeno effect, i.e. the slowing down of the decay rate at any time. Yet, in the opposite case, when the displacement of these energies is larger than the Lorentzian width, the measurement induces an acceleration of the decay rate in the regime of the exponential decay (the anti-Zeno effect). At small times, however, the measurement always slows down the decay rate.

With respect to the energy distribution of the tunneling particle, the measurement always generates strong broadening. However, for very narrow Lorentzian shape of the density of states (the Lorentzian width is smaller than the tunneling amplitude) the effect of the measurement is more peculiar. This takes place where the displacement between the initial energy and the Lorentzian mid-energy is large. Then, if there is no measurement, the energy distribution peaks near the initial state energy, whereas the second peak (near the Lorentzian center) is very weak. However, when the measurement is switched on, the peak at the initial energy disappears with the increase of decoherence, generated by the detector. On the other hand, the second peak near the Lorentzian mid-energy arises.

All these results were obtained without taking into account the coupling of the fermionic quantum dots to the radiation or to the phonon fields. In fact, in a weak coupling regime our treatment can be extended to this case. Yet, we do not expect any essential modification of the results obtained in this paper. The strong coupling regime, however, needs a special consideration.

Our analysis shows different effects generated by continuous measurement. All of them were obtained solely from the time-dependent Schrödinger equation applied to the entire system. Moreover, it looks that some of these effects might be in a contradiction with the projection postulate, which leads to the slowing of the decay rate. Yet, this point deserves special investigation on the level of the macroscopic description of the measuring device. It would involve a proper definition of the measurement time, needed for application of the projection postulate. Although we are not coming to this point in our paper, we nevertheless consider our analysis as a necessary step for a better understanding of the measurement problem and the nature of the projection postulate.

VI. ACKNOWLEDGMENTS

We thank Y. Imry, S. Levit, A. Kofman and G. Kurizki, for valuable discussions. One of us (S.G.) would like to acknowledge the hospitality of Oak Ridge National Laboratory and TRIUMF, while parts of this work were being performed. One of us (B.E.) gratefully acknowledge the support of GIF and the Israeli Ministry of Science and Technology and the French Ministry of Research and Technology

-
- [1] B. Misra and E.C.G. Sudarshan, *J. Math. Phys.* **18** (1977).
 - [2] J. von Neumann, "Mathematical Foundations of Quantum Mechanics," Princeton University Press, Princeton, 1955.
 - [3] A.D. Panov, *Ann. phys. (N.Y.)* **249**, 1 (1996).
 - [4] A. Peres, *Am. J. Phys.* **48**, 931 (1980); P.G. Kwiat, *The Proceedings of the Nobel Symposium (#104) on Modern Studies of Basic Quantum Concepts and Phenomena*, Phys. Scripta, to appear.
 - [5] W.L. Power and P.L. Knight, *Phys. Rev. A* **53**, 1052 (1996).
 - [6] A. Beige and G.C. Hegerfeldt, *J. Phys. A* **30**, 1323 (1997).
 - [7] S. Inagaki, M. Namaki, and T. Tajiri, *Phys. Lett. A* **166**, 5 (1992).
 - [8] G.S. Agarwal and S.P. Tewari, *Phys. Lett. A* **185**, 139 (1994).
 - [9] A.G. Kofman and G. Kurizki, *Phys. Rev. A* **54**, R3750 (1996).
 - [10] S.A. Gurvitz, *Phys. Rev. B* **56**, 15215 (1997).
 - [11] G. Hackenbroich, B. Rosenow, and H.A. Weidenmüller, *Phys. Rev. Lett.* **81**, 5896 (1998).
 - [12] B. Elattari and S.A. Gurvitz, *Phys. Rev. Lett.* **84**, 2047 (2000).
 - [13] K. Hepp and E.H. Lieb, *Helv. Phys. Acta* **46**, 573 (1973).
 - [14] S.A. Gurvitz and Ya.S. Prager, *Phys. Rev. B* **53** (1996), 15932.
 - [15] W.M. Itano, D.J. Heinzen, J.J. Bollinger, and D.J. Wineland, *Phys. Rev. A* **41**, 2295 (1990); C. Presilla, R. Onofrio and U. Tambini, *Ann. of Phys.* **248** 95, (1996), and references therein.
 - [16] R.A. Harris and L. Stodolsky, *Phys. Lett. B* **116** (1982), 464; E. Block and P.R. Berman, *Phys. Rev. A* **44**, 1466 (1991). V. Frerichs and A. Schenzle, *Phys. Rev. A* **44**, 1962 (1991).
 - [17] L. Fonda, G. C. Ghirardi and A. Rimini, *Rep. Prog. Phys.* **41**, 587, (1978).
 - [18] D. Home and M.A.B. Whitaker, *Ann. of Phys.* **258**, 237 (1997).
 - [19] L.S. Schulman, *Phys. Rev. A* **57**, 1509 (1998).
 - [20] A.G. Kofman and G. Kurizki, *Acta Physica Slovaca* **49**, 541 (1999).

- [21] A. D. Panov, Phys. Lett. **A260**, 441 (1999), and references therein.
- [22] Y. Imry, Phys. Scripta **T76**, 171 (1998).
- [23] I. Bar-Joseph and S.A. Gurvitz , Phys. Rev. B **44**, 3332 (1991); S.A. Gurvitz , Phys. Rev. B **44**, 11924 (1991).
- [24] C. Cohen-Tannoudji, J. Dupont-Roc, and G. Grynberg, *Atom-Photon Interactions: Basic Processes and Applications* (Wiley, New York, 1992).
- [25] M.B. Mensky, Phys. Lett. **A257**, 227 (1999).
- [26] R. Landauer, J. Phys. Condens. Matter **1**, 8099 (1989).
- [27] M. Field *et al.*, Phys. Rev. Lett. **70**, 1311 (1993); E. Buks, R. Shuster, M. Heiblum, D. Mahalu and V. Umansky, Nature **391**, 871 (1998).
- [28] S.A. Gurvitz , Phys. Rev. **B57** (1998) 6602.
- [29] J. Bardeen, Phys. Rev. Lett. **6**, 57 (1961).
- [30] In fact, the anti-Zeno effect have been discussed earlier in different publications, for instance [9,10,20] and B. Kaulakys and V. Gontis, Phys. Rev. A **56**, 1131 (1997).